Some Observations Regarding Stochasticity of Dynamic Response of 2D Disordered Brittle Lattices

S. Mastilovic *

Faculty of Construction Management, Union University

Cara Dusana 62-64, 11000, Belgrade, Serbia

ABSTRACT: It had been long recognized that the tensile strength of brittle materials increases with increase of the loading rate. In the present paper, a statistical approach to rupture of a disordered two-dimensional (2D) triangular truss lattice consisting of fragile nonlinear springs is attempted in hope to elucidate some generic effects of structural and geometrical disorder on the tensile strength and the (stress-peak and post-peak) damage energy rates. The simulation results reveal increase of the mean and decrease of the standard deviation of the macroscopic tensile strength with increase of the structural and geometrical order till the "theoretical strength" saturation. At the same time, the increase in lattice disorder results in increase of the mean and standard deviation of the stress-peak damage energy rate, followed by the decrease of the same in the softening regime.

KEY WORDS: discrete models, brittle systems, disorder, dynamic strength, damage energy rate, stochasticity

INTRODUCTION

The study of fracture process in heterogeneous or multi-phase materials remains an active research topic in more than two decades. However, due to subtle interplay of the structural disorder, the dynamically induced nonlinear stress field, and the inherent limitations of the perpetually advancing experimental techniques (Field et al., 2004), the stochastic nature of brittle dynamic response remains difficult to capture theoretically. The significant advances in visualization, characterization, and modeling that are made recently in experimental and computational mechanics (e.g., Zavattieri et al., 2001; Espinosa and Zavattieri, 2003; Zhou and Molinari, 2004; Kraft et al., 2008) outline a promising synergy that appears to be limited only by available computational power. Nonetheless, the use of lattices, as reasonable simplifications of more realistic systems, still has its merits to the extent they can capture "essential properties of fracture"

* Tel.: +381 11 218-0287, e-mail: smastilovic@fgm.edu.rs

(Hansen et al., 1989) that are only weakly dependent on the complexities of realistic systems. These virtual 2D microstructures offer an efficient approach to stochasticity of micro-fracture physics of brittle materials and may shed some light on its connection with macroscopic response. As a consequence, the disordered lattices are used extensively for the last three decades to study various aspects of damage evolution and failure of inhomogeneous or multi-phase systems (e.g., Hansen et al., 1989; Curtin et al., 1997; Mastilovic et al., 2008). The recent advances in statistical damage mechanics rely crucially on the lattice simulations (e.g., Rinaldi et al., 2007, and references therein). A thorough review of lattice models in micromechanics is presented by Ostoja-Starzewski (2002).

The present investigation is a sequel of the analysis of the ordering effect of kinetic energy on dynamic behavior of low-fracture-energy materials (Mastilovic et al., 2008) with emphasis shifted on the influence of structural and geometrical disorder. Those highly brittle materials are characterized with the inferior tensile strength and negligible effects of dislocation activity on dynamic behavior. The lattice simulations are used to investigate stochasticity of high rate response and dynamic failure of these materials. This is achieved by performing repeatedly dynamic tensile test simulations at four strain rates ($\dot{\varepsilon}$ = 10, 1×10^3, 1×10^5, 1×10^7 s^{-1}) spanning the medium-to-high strain rate range with focus on the tensile strength and damage energy rate (i.e., strain energy release rate).

It is inherently difficult to approach objectively the data scatter of the actual dynamic tests since it may be hard to discern between the actual physics and the artifacts of the experimental technique (e.g., dissimilar sample materials, alignments of load platens and sample, etc). The primary advantage of the "virtual experiments" is the ability to exert almost unlimited control over the "test" conditions coupled with the natural introduction of the various types of disorder.

LATTICE SIMULATIONS

The 2D triangular lattice model considered herein is formed by "continuum particles" located at lattice nodes (192 × 227), which interact by nonlinear links characterized by a small tensional rupture threshold (for details refer to Mastilovic et al., 2008, and references therein). The links are very brittle; their critical extension at rupture is ε_{cr} = 0.1%.

The disordered is initially introduced by the normal distribution of equilibrium interparticular distances (λ_0) and the uniform distribution of link stiffness (k). The ranges of these distributions, $\alpha\,\bar{\lambda} \le \lambda_0 \le (2-\alpha)\,\bar{\lambda}$ and $\beta\,\bar{k} \le k \le (2-\beta)\,\bar{k}$, are defined by order parameters α and β, which vary between 0 and 1 and represent measures of divergence from the ideal lattice (α = 1, β = 1). It is often professed that, depending on the observation scale, the geometrical disorder can take into account, for instance, the distribution of grain sizes, while the structural (chemical) disorder encompasses the inherent or induced flaw structure defining the grain boundary cohesive interface of the brittle solid (e.g., Kraft et al., 2008). The reduced-units mean link length ($\bar{\lambda} = 1$) and the mean link stiffness ($\bar{k} = 50$) are arbitrarily selected model parameters.

In general, damage is related to irreversible changes in material and corresponding energy dissipation. Since the micro-fracture is the only dissipative process included in the present model, the link parameters define the damage energy

$$\mathrm{E}_D = \frac{1}{2}\sum k\,\lambda_0^2\,\varepsilon_{cr}^2 \tag{1}$$

tracked throughout simulations, as the cohesive energy released in the course of link ruptures. Since the link stiffness and initial length are stochastic parameters, the damage is "a probabilistic nucleated event" (Curtin et al., 1997) driven by the local stress. The damage energy is reported in this paper normalized, $\overline{\mathrm{E}}_D = \mathrm{E}_D/\mathrm{E}_{D0}$, with the strain energy released upon the rupture of one single bond with average properties, $\mathrm{E}_{D0} = \bar{k}\,\bar{\lambda}_0^2\,\varepsilon_{cr}^2/2$.

The full set of 30 simulations per each loading rate are performed on two lattices characterized by substantially different disorder levels labeled tentatively as:

- Large disorder (*LD*): (α, β) = (0.02, 0.5), and
- Small disorder (*SD*): (α, β) = (0.2, 0.9).[1]

The numerical simulation of the displacement-controlled uniaxial tension test (Figure 1) is designed to ensure uniform distribution of load within a sample and to cancel adverse effects of the lateral inertia (Mastilovic et al, 2008; Mastilovic, 2008) by imposing an initial velocity field (t=0) to *all* lattice nodes:

$$\dot{x}_1(t=0) = \dot{\varepsilon}_1\,x_1 \tag{2a}$$

$$\dot{x}_2(t=0) = -\upsilon_0^{(\varepsilon)}\,\dot{\varepsilon}_1\,x_2 \tag{2b}$$

The initial "velocity kick" is defined by Equations (2) in terms of the prescribed strain rate, $\dot{\varepsilon} = \dot{\varepsilon}_1 = \dot{L}/L$, and the Poisson's ratio $\upsilon_0^{(\varepsilon)} = 1/3$, that is characteristic of the ideal 2D triangular lattice, and corresponds to the Poisson's ratio $\upsilon_0 = 1/4$ of a pristine material. Following the application of the initial velocity field, only velocity of the particles located at the specimen's longitudinal boundaries ($x_1 = \pm L/2$) is controlled

$$\dot{x}_1 = \pm\,\dot{\varepsilon}_1\,L/2, \quad (\forall\, t > 0) \tag{3}$$

[1] The selection of order parameters for the two model sets warrants a disclaimer. The *LD* lattice order parameters were chosen originally (Mastilovic et al., 2008, and references therein) to capture, as close as possible within the limits of the model, the micrographs of alumina. Consequently, the geometrical disorder was maximized while the structural disorder was, in absence of appropriate data, selected arbitrarily to account reasonably for a variety of grain boundary interfacial strengths. The choice of the *SD* lattice order parameters in the present investigation was, to a certain extent, driven by the preceding *LD* selection. The well-documented shortcomings of the strongly disordered lattice (e.g., Jagota and Bennison, 1994; Van Mier and Man, 2009) are important to recognize although they do not affect significantly the qualitative observations of this investigation.

while the motion of all other particles is governed by the Newton's equation of motion.

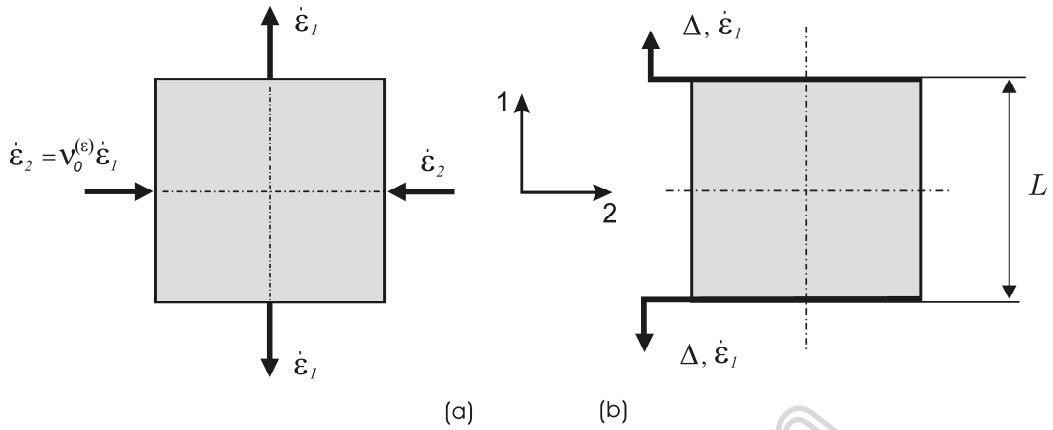

Figure 1. *The uniaxial test simulation set-up; (a) application of the initial strain rate field, (b) displacement-controlled longitudinal tension.*

As a consequence of the initial velocity field applied perpendicular to the loading direction, the stress in the lateral direction is approximately zero regardless of the strain rate of the external load applied in the longitudinal direction (i.e., $\sigma_2 \approx 0, \quad \forall \dot{\varepsilon}$), and all the tests—regardless of the loading rate—are performed under identical in-plane conditions (Mastilovic et al., 2008).

The convergence and mesh objectivity aspects of the model were addressed in literature (as reported by Mastilovic et al., 2008).

SIMULATION RESULTS

The simulations are performed at four different loading rates ($\dot{\varepsilon}$ = 10, 1×10^3, 1×10^5, and 1×10^7 s^{-1}) by using 30 different statistical realizations of the geometrical and structural disorder (reflected by the selection of the pseudo-random-number-generator seed). The basic tensile strength statistics that is presented in Table 1 summarizes the two sets of simulations performed on the models characterized by two different disorder levels (*LD* and *SD*) defined previously. These results are consistent with the experimental observations that suggest that the dynamic tensile strength of brittle materials at high strain rates introduced by shock waves can exceed the quasi-static tensile strength by an order of magnitude (e.g., Grady and Hollenbach, 1979). The simulation results also re-affirm the modest strain-rate sensitivity of brittle materials at lower loading rates for which the tensile strength is dominated by the subcritical crack growth. A single dominant macrocrack evolves from the most "favorably" positioned among weak links, which eventually results in a catastrophic failure at a small macro damage density level. The steep ascent of tensile strength with the loading rate increase (schematically depicted in Figure 3 at two disorder levels) coincides with the transition of fracture pattern from a couple of dominant macrocracks to the web of uniformly distributed microcrack clusters (Mastilovic et al., 2008). It is noteworthy that while stress and

damage energy time histories for low and high loading rates generally reveal the brittle properties of the failure process[2], those in Figure 2, corresponding to this transition, reveal a number of quasi-ductile characteristics; most notably, the relatively significant damage accumulation in the hardening regime and the pronounced softening regime, resulting from the collective behavior of the microcracks comprising the microcrack clouds (Mastilovic et al., 2008). The reduction of tensile strength stochasticity in this strain rate range is attributed to the averaging effect within these clusters (Zhou et al., 2004).

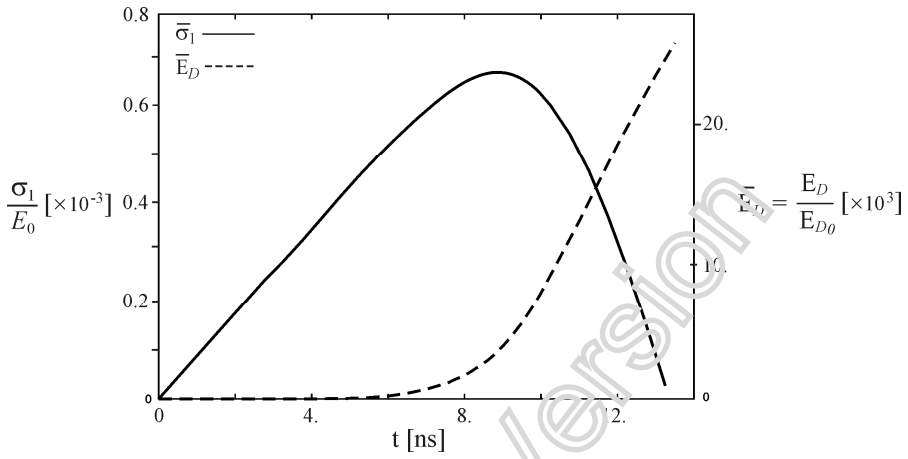

Figure 2. *Typical time histories of stress and damage energy for one realization at* $\dot{\varepsilon} = 1\times10^5$ s^{-1}.

The high-strength plateau (i.e., the upper strength asymptote), labeled provisionally as "theoretical strength" in the forthcoming discussion, corresponds to a completely uniform distribution of microcracks (see the detail in Figure 3) and almost a complete absence of stochasticity. This increasingly deterministic response associated with the extremely high loading rates is attributed to the fact that the propagation of activated and nucleated microcracks, the load redistribution within the brittle system, and the corresponding cooperative phenomena are practically inhibited by inertial effect (Wang and Ramesh, 2004).

The basic statistics of tensile strength data (specifically: the mean, the standard deviation, and the ratio of non-outlier maximum and minimum values) obtained from numerical simulations is presented in Table 1 as the *LD–SD* (large disorder – small disorder) pairs. The results illustrate the effect of geometrical and structural disorder and the loading rate on the tensile strength statistics for the idealized brittle solid. Namely, since the weak links are relatively more abundant in the presence of large disorder, they promote early ruptures and initiation of microcrack clusters. Furthermore, the increased concentration of weak links increases stochasticity of the failure process as reflected by the tensile strength data scatter in Table 1. As a consequence, the strain rate sensitivity for the brittle materials is more pronounced for the large-disorder brittle systems. Specifically, it can be observed from Table 1 that the mean value of tensile strength increases approximately 12 and 4 times from $\dot{\varepsilon} = 10$ s^{-1} to 1×10^7 s^{-1} for *LD* and *SD*, respectively.

[2] The stress increases linearly with time and drops suddenly upon failure with negligible damage accumulation prior to failure.

Thus, in the notation used by Mastilovic et al. (2008)

$$\sigma_m \propto \dot{\varepsilon}^{\varsigma} \tag{4}$$

and the scaling parameter ς is disorder-dependent.

Table 1. *Statistics of the dynamic tensile strength data for the two models characterized by large disorder and small disorder (LD – SD)*

$\dot{\varepsilon}$ [1/s]		1×10^{1}	1×10^{3}	1×10^{5}	1×10^{7}
σ_m/E_0 [$\times10^{-3}$]	MEAN	.0887 – .264	.235 – .343	.482 – .659	1.07 – 1.07
	STANDARD DEVIATION	.0155 – .0148	.0115 – .0152	.00209 – .00183	.00185 – .000780
	MAX.–MIN. VALUE RATIO	1.94 – 1.25	1.32 – 1.17	1.08 – 1.01	1.07 – 1.00

Similarly, the increase of tensile strength with the strain rate can be represented by the following expression

$$\sigma_m = \sigma_{m0} + S_m \left\{1 - \exp\left[-\left(\frac{\log(\dot{\varepsilon}) + A}{B}\right)^C\right]\right\} \tag{5a}$$

where

$$S_m = S_m(\alpha,\beta) = \sigma_m^{th} - \sigma_{m0} \tag{5b}$$

is the measure of hardening, and A, B, and C are fitting parameters, identifiable from the rate-affected strength change. Specifically, Equation (5a) is a mathematical description of the mean tensile strength change with the strain rate, schematically outlined in Figure 3, with the lower and upper strength asymptotes being the quasi-static tensile strength (σ_{m0}) and the theoretical tensile strength (σ_m^{th}), respectively. The discussion of Equations (5) is beyond the scope of the present paper, but it is important to emphasize that Equation (5b) expresses dependence of the rate-driven increase of the tensile strength on the microstructural disorder (e.g., $S_m^{LD} > S_m^{SD}$). The detailed analysis of the functional dependence $S_m = S_m(\alpha,\beta)$, based on the lattice simulation results, would be straightforward but of seemingly dubious use, keeping in mind the highly idealized and simplified character of the virtual 2D microstructure presented herein.

The scatter of strength data for the four loading rates and two material disorder levels, presented in Table 1, is depicted schematically by the shaded areas in Figure 3. The large scatter corresponding to $\dot{\varepsilon}$ = 10 s^{-1} is reduced to a single line at $\dot{\varepsilon}$ = 1×10^{7} s^{-1}, which is indicative of the substantial reduction of the

tensile-strength scatter close to the "upper-plateau" loading rate range. This suggests that the theoretical strength, defining the upper limit strength, is a deterministic property defined primarily by the chemical bonding and relatively insensitive to the subtle features of the material texture (Mastilovic et al., 2008). The evident transition from the stochastic to the deterministic behavior—reflected by the reduction of the strength dispersion and change of damage evolution patterns discussed by Mastilovic et al. (2008)—is more pronounced in the case of the large microstructural disorder. In other words, the uncertainty of the brittle material strength increases with the increase in randomness of microstructure (either geometrical or structural). This behavior can be explained by the increase of importance of complex interplay of microstructural features in the case of relatively narrow range of microstructural disorder (Rinaldi and Lai, 2007).

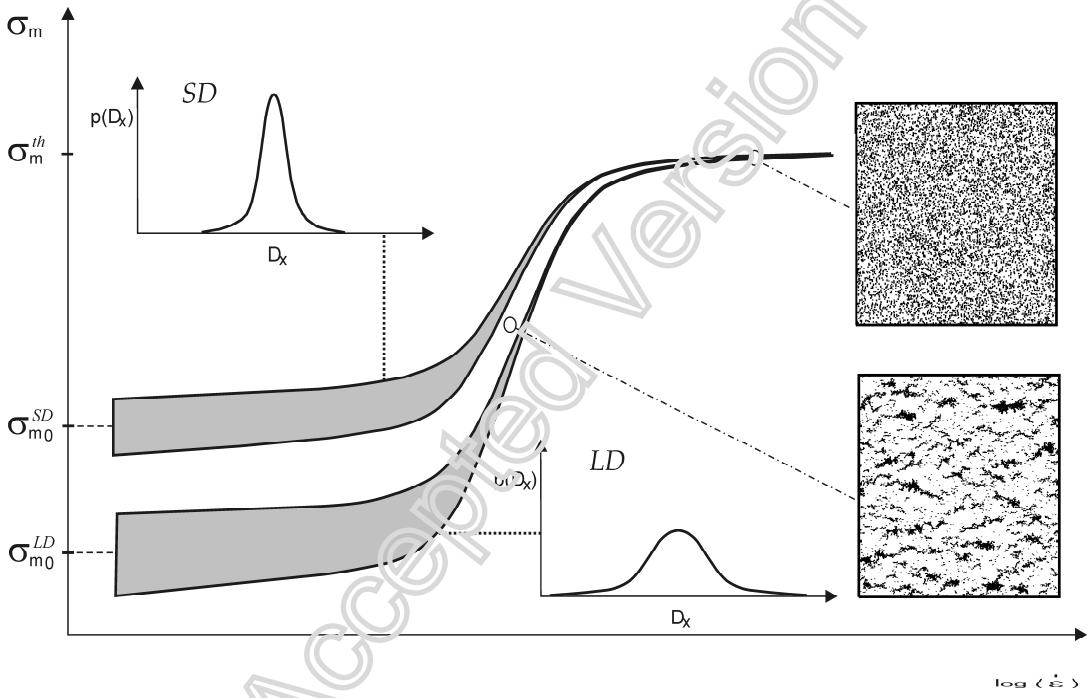

Figure 3. *Schematic representation of the tensile strength dependence on the strain rate indicating the ordering effect of kinetic energy and the effect of geometrical and structural disorder. (Note that the three tensile strengths depicted at the ordinate represent the mean values at the corresponding locations.)*

The importance of the microstructural events that take place at the stress peak that marks onset of localization is worth to emphasize (Van Mier and Man, 2009). The present focus is on the stress-peak and post-peak damage energy rates (Tables 2 and 3, respectively), although the similar observations were made for the scalar damage parameter (damage density). The stress-peak damage energy rate is defined unambiguously, while the post-peak damage energy rate reported herein refers to the maximum damage energy rate in the softening regime (which corresponds to the final deformation phase for the avalanche-type failures, but not necessarily in general).

First, it is interesting to note, from the simulation results presented in Table 2, that for the displacement-controlled tension the mean value of the stress-peak damage energy rate scales reasonably well with the strain rate

$$\dot{\mathrm{E}}_{Dm} \propto \dot{\varepsilon} \tag{6}$$

Second, the increase of geometrical and structural disorder results in increase of both the mean value and the standard deviation of the $\dot{\mathrm{E}}_{Dm}$ data.

Table 2. *Statistics of the damage energy rate at the stress peak at two different levels of model disorder*

$\dot{\varepsilon}$ [1/s]	1×10^{1}	1×10^{3}	1×10^{5}	1×10^{7}	
$\dot{\bar{\mathrm{E}}}_{Dm}\ [\times10^{3}]$	0.0034 / 0.0030	0.27 / 0.25	22. / 1.1	6400. / 900.	**LARGE DISORDER**
MEAN / STAND. DEVIATION	0.0027 / 0.0028	0.22 / 0.10	25. / 1.3	3600. / 680.	**SMALL DISORDER**

Table 3. *Statistics of the damage energy rate in the softening region at two different levels of model disorder*

$\dot{\varepsilon}$ [1/s]	1×10^{1}	1×10^{3}	1×10^{5}	1×10^{7}	
$\dot{\bar{\mathrm{E}}}_{Df}\ [\times10^{3}]$	1.2 / 0.36	2.1 / 0.84	37. / 1.0	11000. / 4200.	**LARGE DISORDER**
MEAN / STAND. DEVIATION	1.3 / 0.56	2.6 / 1.7	55. / 2.1	7600. / 4000.	**SMALL DISORDER**

The basic statistics of the post-peak damage energy rate, presented in Table 3, reveals the opposite disorder effect. Namely, it appears that the higher stress-peak damage energy rates—characteristic of the more disordered model—are followed by the lower post-peak (softening) damage energy rates, both in terms of the mean value and the data scatter.

Strength Limit Case – Small Perturbations of the Ideal Lattice

With the further disorder reduction, the ratio between the upper and lower dynamic strength asymptotes continues to drop. Thus, the low-rate tail of the σ_m vs. $\log(\dot{\varepsilon})$ curve continues to rise, as schematically depicted in Figure 3. For example, for $(\alpha, \beta) = (0.4, 0.95)$, $\sigma_m^{th} / \sigma_{m0} \approx 1.5$.

As a demonstration case of a slightly perturbed ideal lattice, the models corresponding to (α, β) = (0.99, 0.99) are investigated on a smaller sample of 10 statistical realizations. Interestingly, the ratio between the upper and lower tensile strength asymptotes is reduced to 1.4. On the other hand, the strength scatter practically disappears across the whole investigated strain rate range implying that the failure becomes deterministic with the disappearance of disorder.

SUMMARY

The focus of the present inquiry is on the influence of disorder of brittle systems on the stochasticity of their dynamic response.

It is observed that the reduction of microstructural disorder results in reduction of the difference between the upper and lower strength asymptotes, that is, the level of rate-driven material hardening depends on the geometrical and structural uniformity of the material on the spatial scale that dominates the macroscopic response. A strong dependency with grain shape is observed for different microstructures (Zavattieri et al., 2001). Assuming that the larger grain size implies the larger geometrical and structural disorder (e.g., smaller α and β in the present model), one physical explanation of the Hall-Petch relation, in the form expressing the brittle-fracture strength dependence on grain size (Dieter, 1986), may be due to the influence of microstructural disorder on failure process.

The simulation results also suggest that increase in lattice disorder results in increase of both the mean value and the standard deviation of the stress-peak damage energy rate. It appears that the average rate of energy dissipation at the onset of localization scales reasonably well with the strain rate, but additional work seems necessary to confirm this proposition. It is demonstrated that data scatter of the tensile strength and the corresponding damage energy rate are reduced with reduction of geometrical and structural disorder, which implies that the stochasticity of material (e.g., the grain shape and size) advances the stochasticity of its dynamic response at the threshold of softening. On the other hand, the softening phase is characterized by the decrease of the average damage energy rate ($\dot{E}_{Df}$) and the data scatter with increase of geometrical and structural disorder.

REFERENCES

Curtin, W.A., Pamel, M., and Scher, H. (1997). Time dependent damage evolution and failure in materials. II Simulations. *Phys. Rev. B* **55** (18): 12052-12061.

Dieter, G.E. (1986). Mechanical Metallurgy. McGraw-Hill, New York, pp. 189-191.

Espinosa, H.D. and Zavattieri, P.D. (2003). A grain level model for the study of failure initiation and evolution in polycrystalline brittle materials. Part I: Theory and numerical implementation. *Mech. Mater.* **35**: 333-364.

Field J.E., Walley S.M., Proud W.G., Goldrein H.T., Siviour C.R. (2004). Review of experimental techniques for high rate deformation and shock Studies. Int. J. Impact Eng. **30**: 725-775.

Grady, D.E. and Hollenbach, R.E. (1979). Dynamic fracture strength of rock. *Geophys. Res. Letters* **7**: 73-76.

Hansen A., Roux S., Herrmann H.J. (1989). Rupture of central-force lattices. *J. Phys. France* **50**: 733-744.

Jagota A. and Bennison S.J. (1994). Spring-Network and Finite-Element Models for Elasticity and Fracture, in: Bardhan, K.K., Chakrabarti, B.K., Hansen, A. (Eds.), Proceedings of a workshop on breakdown and non-linearity in soft condensed matter, Springer-Verlag Lecture Notes in Physics, Berlin, pp. 186-201.

Kraft, R.H., Molinari, J.F., Ramesh, K.T., and Warner D.H., (2008). Computational micromechanics of dynamic compressive loading of a brittle polycrystalline material using a distribution of grain boundary properties. *J. Mech. Phys. Solids* **56**: 2618-2641.

Mastilovic S., Rinaldi A., and Krajcinovic D. (2008). Ordering effect of kinetic energy on dynamic deformation of brittle solids. *Mech. Mater*. **40** (4-5): 407-417.

Mastilovic S. (2008). A Note on Short-Time Response of Two-Dimensional Lattices During Dynamic Loading. *Int. J. Damage Mech*. **17**: 357-361.

Ostoja-Starzewski M. (2002). Lattice models in micromechanics. *Appl. Mech. Rev*. **55** (1): 35-60.

Rinaldi A, Krajcinovic D., Mastilovic S. (2007). Statistical Damage Mechanics and Extreme Value Theory. *Int. J. Damage Mech*., **16**: 57-76.

Rinaldi A, Lai Y-C. (2007). Damage Theory of 2D Disordered Lattices: Energetics and Physical Foundations of Damage Parameter. *Int. J. Plasticity*, **23**: 57-76.

Van Mier, J.G.M and Man, H. (2009). Some Notes on Microcracking, Softening, Localization, and Size Effect. *Int. J. Damage Mech*., **18 (3)**: 283-309.

Wang, H. and Ramesh, K.T. (2004). Dynamic strength and fragmentation of hot-pressed silicon carbide under uniaxial compression. *Acta Mater.* **52**: 355-367.

Zavattieri, P.D., Raghuram, P.V., and Espinosa, H.D. (2001). A computational model of ceramic microstructures subjected to multi-axial dynamic loading. *J. Mech. Phys. Solids* **49**: 27-68.

Zhou, F. and Molinari, J.F. (2004). Stochastic fracture of ceramics under dynamic tensile loading. *Int. J. Solids Struct*. **41**: 6573-6596.